# STUDY OF THE IMPACT OF RUBBER CYLINDERS ON ALUMINUM PLATES

**Priscila Porr, priscila.porr@poli.usp.br**
**Larissa Driemeier, larissa.driemeier@poli.usp.br**
Departamento de Engenharia Mecatrônica e Sistemas Mecânicos. Escola Politécnica da Universidade de São Paulo
Av. Prof. Mello Moraes, 2231. 05508-900 Sao Paulo, S.P. Brazil

***Abstract.*** *The study of ballistic impact has many practical applications. Particularly, in aeronautical engineering the impact of small debris on the airplane structures, including small tire, asphalt and fuselage fragments, can cause financial, structural and human safety damages. The aim of this study is to obtain a numerical modeling for the ballistic limit of the impact of a tire fragment on an aluminium plate. Rubber specimens were obtained from a Dunlop aeronautical tire and the aluminum alloy is typical for aeronautical applications. Material's properties were obtained through the inverse technique, that is, parameters are determined correlating experimental and numerical data. The theoretical approach emphasizes the study of material's modeling and failure criteria. For the aluminum and rubber, Lemaitre' continuum damage model and Mooney-Rivlin model were used, respectively. Experimental impact tests were conducted with a gasgun. The model is validated through comparisons between numerical and experimental results.*

***Keywords****: impact, nonlinear numerical simulation, experimental tests.*

## 1. INTRODUCTION

The aim of the present work is to study the impact of soft bodies on flat aluminum plates. The study of ballistic impact has many practical applications, such as military, mining and construction technology, nuclear reactors etc. Particularly concerning aeronautical engineering, the impact of small debris, such as small tire, asphalt and fuselage fragments, on airplane's structure can cause great financial, structural and human safety damages.

The most well known accident involving impact of small objects on airplanes happened on the 25th July 2000 in Paris with the Concorde, leaving a total of 113 deaths. According to French Government's report (2000), the accident was caused by fragments of Concorde's tires, which were damaged during takeoff. These fragments were accelerated to a very high velocity, and were thrown against the aircraft's structure, damaging the wing and the left turbine, which failed during takeoff. Consequently, the airplane lost lift after flying few hundred meters. Numerical studies of this impact can be found in the literature (Mines et al. 2006; Karagiozova and Mines, 2006).

The analysis of such structure under impact loading involves, usually, complex geometries, great strains, plasticity, temperature variation, inertia effects and material separation, among other phenomena. Therefore, it is one of the most complex phenomena of structural engineering.

However, due to its complexity and to the high costs of experimental tests, beyond the fact that there are few laboratories able to do such tests, it is not viable to base a whole study only on experimental tests. Thus, in this study, the theoretical, numerical and experimental approaches were developed concomitantly.

The theoretical approach emphasizes the study of material's modeling and failure criteria. The plate's aluminum is characterized according to Lemaitre damage model. Besides, rubber specimens were obtained from a used Dunlop aeronautical tire. The most usual method for rubber characterization is Mooney-Rivlin model.

The experimental approach deals with materials' characterization (aluminum and rubber) and with ballistic tests in aluminum plates. Concomitantly, these tests have been numerically modeled in finite elements. For material's characterization it was used the inverse technique, in which material's properties are determined correlating numerical and experimental data. Nowadays, this method is commonly used in the literature – see, for example, Pickett et al. 2004.

Finally, for material's characterization and model's validation, experimental impact tests were numerically simulated in a commercial FE software LS-Dyna.

## 2. MATERIALS AND METHODS

### 2.1. Material modeling

Lemaitre damage model was used, including a critical damage value for failure criteria.

### 2.1.1. Elastoplastic models for aluminum

Although there are numberless material models in literature nowadays, models that do not require complex material's characterization are always the most used ones. Among these are von Mises model, Johnson and Cook (1983) and Lemaitre damage model (Lemaitre, 1985).

Very briefly, shear-energy theory or von Mises-Henky theory is the most widely known theory for ductile materials, and it can be found in classic literature (Shigley et al. 2005). This theory is based on the observation that, in ductile materials under hydrostatic stresses, the yield strength was much greater than the values obtained in simple tensile tests. It was then postulated that yield is not a simple tensile or compressive stress phenomenon, but it is somehow related to the angular distortion of the stressed element.

Johnson and Cook theory is more sophisticated; it includes strain rate and temperature effects, and proposes a particular failure criteria. The model is widely used in impact tests – see, for example, Borvick et al – since it is reasonably efficient. Johnson and Homlquist (1989) found the parameters for many materials used in the engineering field.

### Lemaitre damage model

This continuum damage model was proposed by Lemaitre (1985), as following:

$$\dot{D} = \begin{cases} 0 & \bar{\varepsilon}^{p} \leq \bar{\varepsilon}^{p}_{crit} \\ \dfrac{Y}{S(1-D)}\dot{\varepsilon} & \bar{\varepsilon}^{p} > \bar{\varepsilon}^{p}_{crit} \end{cases} \tag{3}$$

$$Y = \frac{\sigma_{eq}^{2}}{2E} R_{v} \tag{4}$$

$$R_{v} = \frac{2}{3}(1+\nu) + 3(1-2\nu)\zeta^{2} \tag{5}$$

where $D$ is the material damage ($D=0$ when the material is not damaged, $D=1$ when the material breaks), $E$ is the Young's modulus and ν is Poisson's ratio. Damage evolution occurs when accumulated plastic strain $\bar{\varepsilon}^{p}$ exceeds a critical value $\bar{\varepsilon}^{p}_{crit}$. The parameter $S$ is a material constant.

### 2.1.2. Hyperelastic models for rubber

In elastic models, the relation between stress and strain is generally defined introducing some elastic constants, since strains are small (Hooke's law). For homogeneous, isotropic materials, an appropriate choice for these parameters is the modulus of elasticity E and Poisson's ratio ν.

Nevertheless, when the material is under high strain levels and the deformations are still reversible – hyperelastic materials, such rubber and other elastomers, biological tissues, etc. – Hooke's law is not a realistic model. In these situations, it is interesting to introduce a scalar function, which depends on the deformation's parameters, to represent material's elastic deformation energy *W*. The relation between stress and strain can be obtained through the derivation of this function *W*, which generally refers to the non-deformed material's configuration.

Two general and experimentally validated expressions for the deformation energy are given by Mooney-Rivlin's expression for incompressible materials (e.g. rubber), and by Blatz-Ko's expression for compressible materials (e.g. foams).

### Mooney-Rivlin model

Melvin Mooney and Ronald Rivlin proposed this material model in two independent papers, in 1952. From experimental observations, Mooney and Rivlin defined a simple, but efficient, functional for the deformation energy in real rubber materials. The model covers many practical interest situations.

$$W = A(I-3) + B(II-3) + C(III^{-2}-1) + D(III-1)^{2} \tag{6}$$

$$C = 0,5A + B \tag{7}$$

$$D = \frac{A(5\nu-2) + B(11\nu-5)}{2(1-2\nu)} \tag{8}$$

In which $2(A+B)$ is the shear modulus in linear elasticity and $I$, $II$ and $III$ are the invariants of Cauchy-Green right tensor $C$. The constants $A$, $B$ can be obtained from a stress-strain curve of a uniaxial compression test.

### 2.2. Failure theories

Failure theories, in the context of this work, aim to predict crack initiation and propagation in the material. There is not any universal failure theory for all materials in any three-dimensional load configuration. In fact, failure theories are based on many different criteria (maximum tensile/compression stress, maximum shear stress, maximum strain energy, etc) and their applications depend on the material, on the loading conditions and on the geometry, among other factors. The hypotheses adopted in each theory have been tested through the years, leading to nowadays accepted practices. The most widely known failure criteria for ductile materials will be analyzed here.

**Accumulated equivalent plastic strain theory**

This is the most simple failure criterion existing, and it assumes that failure occurs when the accumulated plastic strain $\bar{\varepsilon}^p$ reaches a critical value $\bar{\varepsilon}_f$.

$$\bar{\varepsilon}^p = \bar{\varepsilon}_f \tag{9}$$

The accumulated plastic strain is defined as:

$$\bar{\varepsilon}^p = \int_0^t \dot{\bar{\varepsilon}}^p \, dt \tag{10}$$

$$\bar{\varepsilon}^p = \sqrt{\frac{2}{3}\dot{\varepsilon}^p \cdot \dot{\varepsilon}^p} \tag{11}$$

Although this is a widely used criterion and despite the fact that it can be found in almost every finite elements commercial code, this failure criterion dates from the beginning of the 20th century, and its very simplified theory is not suitable for the current non-linear methods.

**Maximum shear stress theory**

Also known as Tresca or Guest's theory, this is an easy-to-use theory that gives good results. This theory says that failure will occur when maximum shear stress in any mechanical element equals or exceeds the maximum shear stress in a specimen of the same material in a tensile test, when it fractures. In mathematical terms, yield begins when:

$$\tau = \frac{\sigma_1 - \sigma_3}{2} \geq \frac{\sigma_{rup}}{2} \tag{12}$$

where $\sigma_1 > \sigma_2 > \sigma_3$ are the principal stresses.

**Johnson-Cook theory**

Johnson-Cook criterion postulates that material failure occurs when accumulated plastic strain reaches a critical value:

$$\bar{\varepsilon}^p = A + Be^{C\zeta} \tag{13}$$

where $\zeta=\sigma_h/\sigma_{eq}$ is the triaxiality of the material, $\sigma_h = (\sigma_1+\sigma_2+\sigma_3)/3$ is the hydrostatic stress and $\sigma_{eq}$ is von Mises equivalent stress.

**Lemaitre critical damage theory**

Lemaitre critical damage theory is based on the evolution of the damage variable. It establishes that the material fractures when the value of the damage $D$ reaches the critical value $D_{crit}$. For ductile materials like aluminum, this value is $0{,}120 \leq D_{crit} \leq 0{,}250$.

### 2.3. Numeric formulations

There are some different formulations to solve problems with finite elements analysis. Some of the most important methods are:

### Lagrangean formulation

Lagrangean formulation is generally used in problems where the solids are barely deformable. In this formulation, every particle’s movement is observed in time and space, and the mesh follows material’s movements, getting distorted as the material is loaded (Fig. 1).

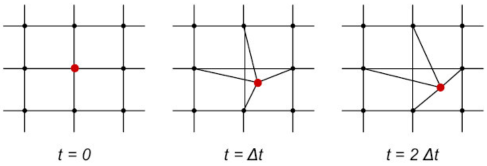

Figure 1. Lagrangean formulation

### Eulerian formulation

Eulerian formulation consists in observing the nodes in space, not following material’s particles movements. In this way, the mesh doesn’t move or get deformed. After each time step, the analysis stops and the following steps are taken (Fig. 2):

- “smoothing”: all nodes whose position was altered due to loading are moved back to their original position;
- “advection”: the internal variables, like stresses and velocities, are recalculated for all displaced nodes, in order to maintain the same spatial distribution as it was before the mesh was “smoothed”.

This formulation is used in fluid analysis.

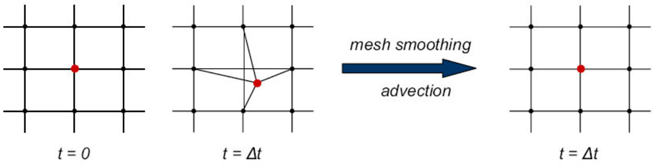

Figure 2. Eulerian formulation

### 2.3.3. ALE formulation

ALE formulation (Arbitrary Lagrangean-Eulerian) mixes both Lagrangean and Eulerian formulations. Differently from Eulerian formulation, in which the nodes are moved back to their initial position, in ALE formulation the nodes are moved back to an intermediate position, calculated according to the average distance from the surrounding nodes.

The advantage of using ALE formulation is to reduce simulation costs by time-step and allow higher strain states.

An ALE timestep (Fig. 3) consists of:

- a Lagrangean timestep;
- nodes are moved back to an intermediate position;
- node’s properties are recalculated.

The number of properties to be calculated depends on the adopted material model. The most simple strategy to lower simulation costs is to use ALE formulation only in some timesteps. In other words, Lagrangean formulation is used, and ALE formulation is used only after a determined number of Lagrangean timesteps. Referring to the computational time, using ALE formulation isn’t viable unless 20% of material’s volume is transported.

ALE formulation is suitable for those cases where the structural shape is highly deformed, once the mesh would be very distorted if Lagrangean formulation was used, leading to numerical errors.

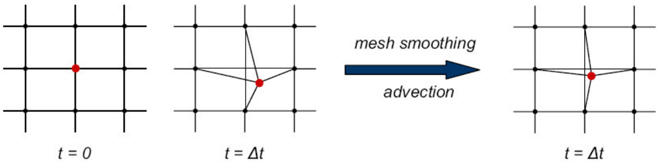

Figure 3. ALE formulation

## 3. RESULTS AND DISCUSSION

### 3.1. Target's characterization

According to Fig. 4, the target used in experimental tests is a commercial aluminum plate with dimensions 0,5 x 350 x 350mm, with a deformable circular area of 250mm diameter.

(a) (b)

Figure 4. Picture of the target for experimental tests

Uniaxial tensile tests were carried out to determine material characteristics. The specimens were machined from a 0,5mm-thick commercial aluminum plate and their dimensions are according to ASTM standard for tensile tests. All tests were performed in an Instron machine model 3369 with load capacity of 50kN (see Fig. 4b). The imposed displacement rate during the quasi-static experiments was 2,0mm/min. Load and displacements were recorded.

Adjusting materials parameters in the numerical simulation of tensile test, the curve obtained numerically shall approximate the one obtained experimentally. The experimental and numerical curves are shown in Fig 5. Material parameters for damage model are presented in Tables 1-2.

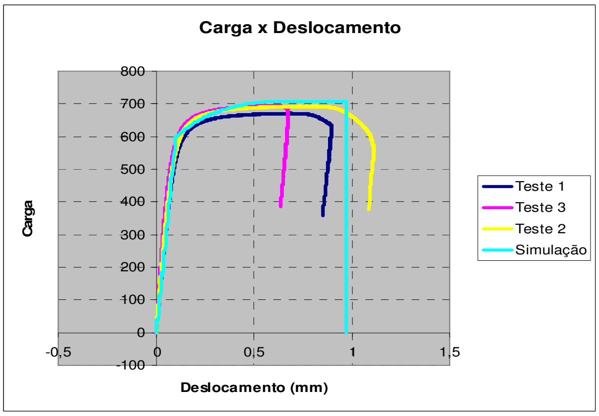

Figure 5. Numerical and experimental load-displacement curve of aluminum tensile tests

Table 1. Elastic material parameters for aluminum, according to Lemaitre's damage model

| Elastic Properties | Value |
|---|---|
| Density (t/mm$^3$) | 2,73.10$^{-9}$ |
| Poisson | 0,35 |
| Elasticity modulus (MPa) | 66,4 |
| Yield stress (MPa) | 120 |

Table 2. Lemaitre's damage material model parameters for aluminum

| Material parameters | Value |
|---|---|
| S (MPa) | 0,6 |
| Critical damage | 0,5 |

### 3.2. Projectile's characterization

Rubber specimens were machined from the rubber of a used Dunlop aeronautical tire. Essentially, an aeronautical tire has a reinforced region and a rubber-rich region. The reinforcement is composed of nylon cords, which are displayed on 16 layers on a natural rubber matrix.

Uniaxial compression tests were held to obtain material's properties. The specimens were cylinders with 25mm diameter and 17mm height. The tests were held with a constant velocity of 0,5mm/min. Table 3 summarizes Mooney-Rivlin parameters for the rubber. Figure 6 shows the numerical and experimental results.

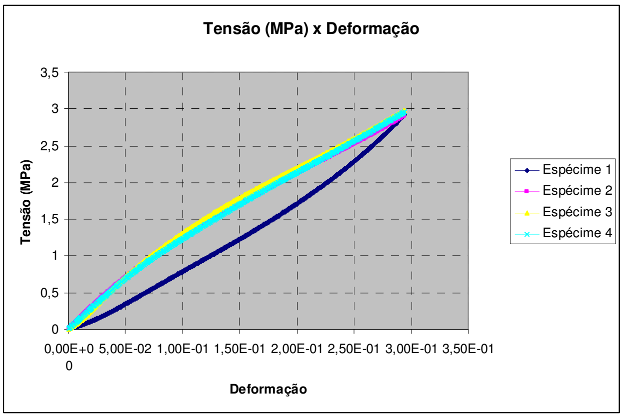

Figure 6. Graphic stress x strain of the rubber compression tests

Table 3. Material parameters for the rubber, according to Mooney-Rivlin model

| Elastic Properties | Value |
|---|---|
| Density (t/mm$^3$) | 8,93x10$^{-10}$ |
| Poisson | 0,495 |
| A (MPa) | 11,45 |
| B (MPa) | 3,22 |

### 3.3. Experimental impact tests

Figure 7 shows a projectile and a sabot. Sabots are cylinders made with nylon, with a hole that holds the rubber projectile.

Figure 7. Picture of a sabot and a rubber specimen

The gasgun is shown in Fig. 8. The equipment is composed by a gas tank that bears up to a pressure of 8bar, an 8-meters long PVC pipe and a velocity sensor at the end of the pipe. Sabot and projectile are firmly positioned near the gas tank, to avoid big pressure losses. A control panel switches the compressor on, and when the pressure achieves the desired level, the shot can be triggered. A chronoscope is used for velocity measurement.

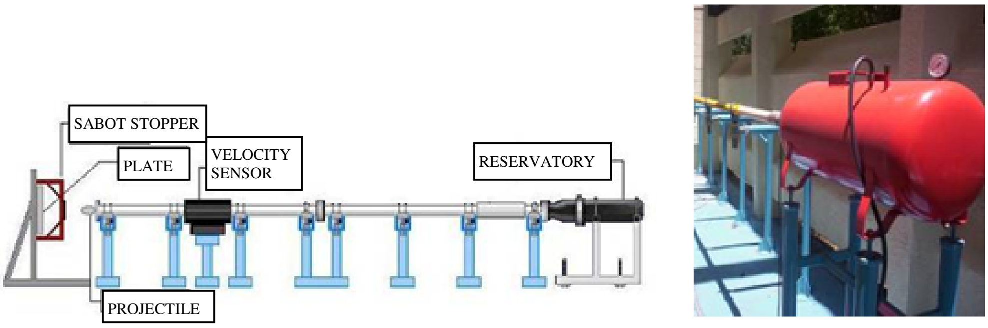

(a) (b)

Figure 8. (a) Gasgun's layout, (b) external view

Experimental impact tests of rubber projectiles on aluminum plates were held on different velocities, in order to determine plate's ballistic limit. Ballistic limit is the lowest projectile's velocity that totally perforates the plate.

Figures 9-11 illustrate plates after the impact of rubber projectiles on different velocities. It can be seen that the ballistic limit of the aluminum plates is between 76m/s and 86m/s, once at 76m/s the projectile only deforms the plate, while at 86m/s it totally perforates the plate.

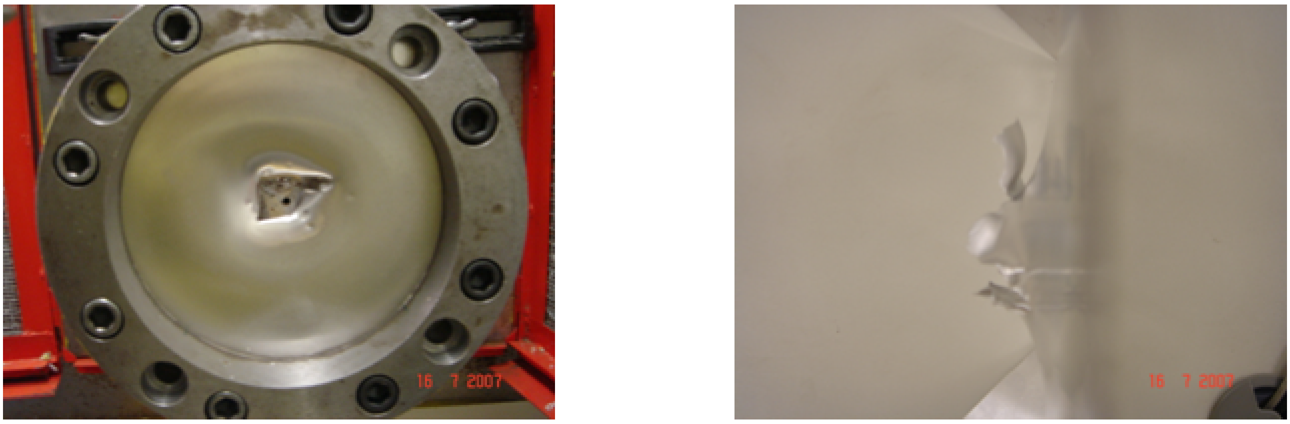

Figure 9. Aluminum plate after impact at a projectile's velocity of 145m/s

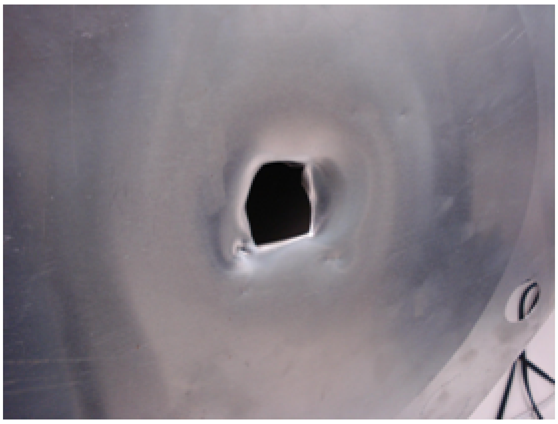

Figure 10. Aluminum plate after impact at a projectile's velocity of 86m/s

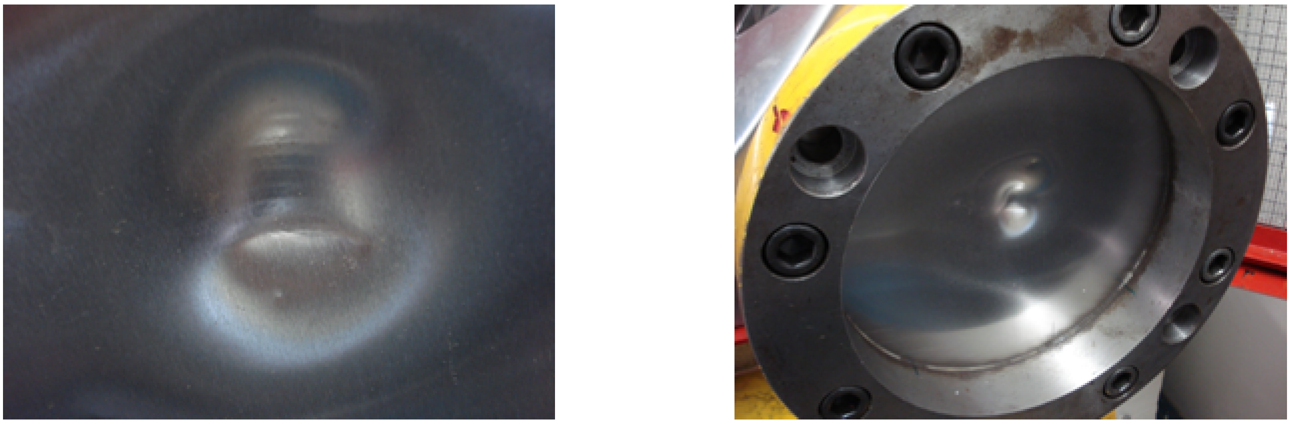

Figure 11. Aluminum plate after impact at a projectile's velocity of 76m/s

### 3.4. Numerical impact simulation

The impact of rubber cylinders on aluminum plates was numerically simulated in the software LS-Dyna®. In the software Hypermesh®, a 250mm-diameter plate was created, which corresponds to the deformable area of the plate used in the experiment. As already discussed, Lemaitre's damage model and Mooney-Rivlin model were used for plate and projectile, respectively. ALE formulation was used for the rubber.

Numerical impact simulations were also performed for different velocities. The highest values of stress occur in the center of the plate (where the cylinder hits the plate) and, for higher velocities, on the borders of the plate, where it is clamped.

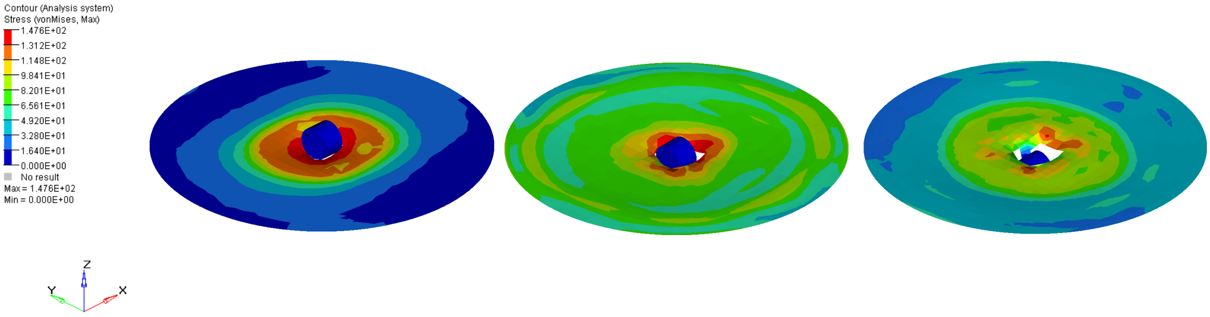

Figure 12. Stress levels on aluminum plate during impact at 60m/s

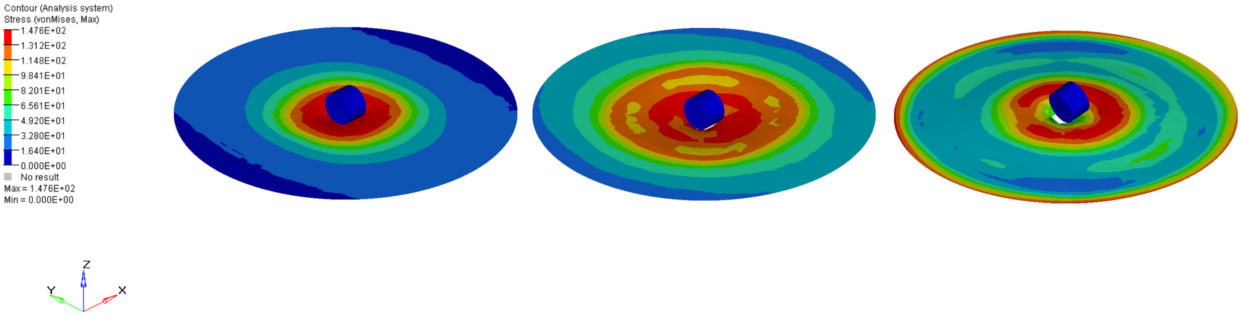

Figure 13. Stress levels on aluminum plate during impact at 50m/s

Based on the images of Fig. 13, the ballistic limit obtained numerically is between 50m/s and 60m/s. At 60m/s, the plate is totally perforated, while at 50m/s the plate is damaged, but not totally perforated.

## 4. CONCLUSIONS

The present work presents three different approaches of a structural analysis: theory, experiments and numerical analysis.

In the first part of this work, material models used in numerical simulations were studied. The materials used in experimental simulations were characterized through the inverse technique, and parameters were used in ballistic limit analyses.

The ballistic limit obtained through experimental tests was in the range of 76–86m/s, against value range of 50–60m/s obtained through numerical analysis.

The discrepancies of the experimental and numerical results have some possible reasons:

- Aluminum dynamic behavior: the aluminum was statically characterized, not considering the effects of strain rates. A more comprehensive study should include dynamical tests on the aluminum. Besides, the damage model used requires a loading and unloading test for its complete characterization. In this way, the parameter S was obtained from the literature.
- Rubber's behavior: although Mooney-Rivlin model is widely used in hiperelastic materials, it has only few parameters, not allowing a precise material characterization.
- Experimental measurements: the ballistic velocity is measured before the projectile leaves the sabot, and there is, probably, energy loss in this detachment, causing a decrease in projectile's velocity.

## 5. REFERENCES

Børvik, T., Dey, S., Clausen, A.H. 2006.“ A preliminary study on the perforation resistance of high-strength steel plates”, J. Phys. IV France, Vo. 134, pp. 1053–1059.

Lemaitre, J. A continuum damage model for ductile fracture ASME Journal of Engineering Materials and Technology, 1985.

Johnson G.R., Cook W. H. A constitutive model and data for metals subjected to large strains, high strain rates and high temperatures in Proc. 7th Int. Symp. Ballistics, The Hague, Netherlands. (1983) 541–547.

Johnson G.R., Homlquist T. J. Test data and computational strength and fracture model constants for 23 materials subjected to large strain, high-strain rates, and high temperatures in Tech. rep. LA-11463-MS, Los Alamos National Laboratory (1989).

Karagiozova, D.; Mines, R. A. W. Impact of aircraft rubber tire fragments on aluminum alloy plates: II – Numerical simulation using LS-Dyna, 2006.

Mines, R. A. W.; McKown, S.; Birch, R.S. Impact of aircraft rubber tire fragments on aluminum alloy plates: I – Experimental, 2006.

Ministere de l'equipament des transports et du logement. Relatório ínterim BEA f-sc000725ae, 2000.

Pickett A.K., Pyttel T., Payen F., Lauro, F., Petrinic N., Werner H., Christlein J. Failure prediction for advanced crashworthiness of transportation vehicles Int. J. Impact Engng., 2004.

Shigley, Joseph E.; Mischke, Charles R.; Budynas, Richard G. Projeto de engenharia mecânica, 2005.

## 6. RESPONSIBILITY NOTICE

The authors are the only responsible for the printed material included in this paper.